



ELSEVIER

Journal of Crystal Growth 208 (2000) 746–756

JOURNAL OF **CRYSTAL
GROWTH**

www.elsevier.nl/locate/jcrysgro

Similarity solutions describing the melting of a mushy layer

Daniel L. Feltham^a, M. Grae Worster^{b,*}

^a*Department of Chemical Engineering, Institute of Science and Technology, University of Manchester, P.O. Box 88, Manchester M60 1QD, UK*

^b*Institute of Theoretical Geophysics, Department of Applied Mathematics and Theoretical Physics, University of Cambridge, Silver Street, Cambridge CB3 9EW, UK*

Received 27 March 1999; accepted 20 August 1999

Communicated by D.T.J. Hurle

Abstract

A model of the melting of a mushy region in the absence of fluid flow is presented. Similarity solutions are obtained which are used to describe melting from a hot plate with and without the generation of a completely molten region. These solutions are extended to describe the melting of a mushy region in contact with a hot liquid. A significant feature of melting mushy regions is that the phase change occurs internally by dissolution. Our solutions for melting of a mushy region are used to investigate this internal phase change and are compared with the classical Neumann solutions for melting of a pure substance. © 2000 Elsevier Science B.V. All rights reserved.

1. Introduction

A mushy region is a mixture of solid and liquid elements coexisting in thermodynamic equilibrium and typically takes the form of a porous matrix of the solid phase bathed in interstitial liquid. Mushy regions form in a variety of alloys such as iron–carbon (steel), copper–zinc (brass) and salt solutions such as sodium–chloride–water. The convoluted geometry of a mushy region is created by morphological instabilities that enhance the expulsion of one or more components from the solid phase as it grows. These instabilities are typically caused by constitutional supercooling, which is due

to the large difference in the diffusion rates of heat and the components of the alloy. A discussion of mushy layers with many examples of where they occur may be found in Ref. [1].

There have been many studies of *solidifying* mushy regions [2]. By contrast, we present a fundamental study of a *melting* mushy layer owing to internal dissolution. Dissolution is driven by thermodynamic disequilibrium resulting from compositional variations, and is rate limited by compositional diffusion. Melting, resulting from thermal disequilibrium, proceeds much more rapidly, at a rate dictated by heat transfer [3]. Within a mushy layer, internal dissolution tends to keep the interstitial concentration on the local liquidus by solute transport on the microscale of the internal morphology. On the macroscale, therefore, the change of phase from solid to liquid is still controlled by rates of heat transfer. We shall, therefore,

* Corresponding author. Fax: +44-1223-337918.
E-mail address: grae@ese.cam.ac.uk (M.G. Worster)

refer to phase change on the macroscopic scale, as melting (or freezing) though it is to be understood that the change of phase on the microscale is due to diffusion of solute. Depending upon conditions, melting of a mushy layer can create a completely molten region or simply reduce its solid fraction. A significant issue is the extent to which partial as opposed to complete melting takes place. Internal phase change plays an important role in fields as diverse as the reprocessing of composite materials, heat transfer during welding, and to the seasonal melting of sea ice.

We restrict our attention to binary alloys since this simplifies the mathematical description of the mushy layer, and, in any case, the behaviour of alloys is often dominated by two major components. We obtain similarity solutions which can be used to describe the melting of a mushy layer when heat and mass transport is effected solely by diffusion.

In Section 2, we introduce the mathematical model and describe the various assumptions we make in order to simplify the analysis and avoid details that are extraneous to the fundamental processes. In Section 3, we use our model to determine similarity solutions that describe how a mushy layer is melted from a hot plate with and without generation of an entirely molten region. In Section 4, we extend these solutions to describe how a mushy layer in contact with a hot liquid may melt. The solutions that we present are extensions to binary alloys of the Neumann solution [4], of the classical Stefan problem for melting. In Section 5, we use our solutions to investigate the extent of internal phase change within the mushy layer and compare our results with those for the melting of a pure substance. The possible implications of internal dissolution are briefly explored using the example of sea ice. Section 6 summarises our main conclusions.

2. Mathematical formulation

We consider the melting of a simple binary eutectic. Without loss of generality, we formulate the problem for the case that the bulk composition of the alloy is less than the eutectic composition. We

assume that the liquidus is linear,

$$T = T_L(C) = T_0 - \Gamma C, \quad (1)$$

where T_0 and Γ are positive constants, and that the solidus is equal to zero. A more detailed description of the model we now introduce can be found in Ref. [5]. Within a mushy zone the alloy consists of a mixture of solid and liquid elements coexisting in thermodynamic equilibrium. In the absence of fluid flow, local conservation of heat can be expressed by

$$[\rho_s c_s \phi + \rho_l c_l (1 - \phi)] \frac{\partial T}{\partial t} = \nabla \cdot (k_m \nabla T) + \rho_s \mathcal{L} \frac{\partial \phi}{\partial t}, \quad (2)$$

where the variables $\phi(\mathbf{r}, t)$ and $T(\mathbf{r}, t)$ represent the locally averaged solid fraction and temperature, respectively, \mathbf{r} is a position vector in the mushy layer and t is time. The latent heat released as liquid solidifies is \mathcal{L} per unit mass of solid, the densities of the liquid and solid are ρ_l and ρ_s , and the specific heat capacities of the liquid and solid are c_l and c_s respectively. The thermal conductivity of the mushy layer is approximated by

$$k_m = \phi k_s + (1 - \phi) k_l, \quad (3)$$

where k_l and k_s are the thermal conductivities in the liquid and solid, respectively. This expression is exact for a parallel laminated medium in the case that the heat flux is aligned with the lamellae [6]. Local conservation of solute can be written

$$(1 - \phi) \frac{\partial C}{\partial t} = \nabla \cdot (D_m \nabla C) + (C - C_s) \frac{\partial \phi}{\partial t}, \quad (4)$$

where $C(\mathbf{r}, t)$ represents the locally averaged concentration of the interstitial liquid, C_s is the composition of the solid formed due to freezing, and D_m is the solute diffusion coefficient in the mushy layer. For the sake of clarity, we assume that the thermal conductivities of the solid and liquid elements of the mushy layer are identical and equal to the constant k ; thus $k_m = k$. Since diffusion of the solute within the solid phase is neglected, $D_m = (1 - \phi)D$, where D is the solute diffusion coefficient in the liquid. We assume that local thermodynamic equilibrium prevails within the mushy layer. This is justified provided that the rate of phase change within the mushy layer is sufficiently

slow that thermodynamic equilibrium can be maintained between the solid elements. This is satisfied if the timescale of solute transport interstitially, δ^2/D , where δ is the solid-element spacing in the mushy layer, is short compared to the timescale of temperature variations within the mushy layer. During the freezing of a mushy layer, solute transport is enhanced by the side-branching of dendrites resulting from morphological instabilities, which reduces δ . During melting, however, δ corresponds to the primary dendrite spacing and the condition is more restrictive. When similarity solutions apply, the heating rate scales with the elapsed time t and thermodynamic equilibrium is therefore maintained once $t \gg \delta^2/D$. In a typical metallic mushy layer, with $\delta \approx 3 \times 10^{-4}$ m and $D \approx 3 \times 10^{-9}$ m²s⁻¹ [7], we expect thermodynamic equilibrium to be maintained after about 30 s. For mushy layers of ice crystals formed from aqueous solutions of sodium chloride, for example, $\delta \approx 10^{-3}$ m and $D \approx 10^{-9}$ m²s⁻¹ so that thermodynamic equilibrium is maintained after about 1000 s. This time is still small compared to the timescales of variation in various applications such as the diurnal variations within a sea-ice layer on the polar oceans [8].

The Lewis number $Le = \kappa/D$ of liquids and solids is very much greater than unity; for example, $Le \approx 100$ in aqueous solutions. This means that, though solutal diffusion ensures local thermodynamic equilibrium between the solid elements, since the macroscopic lengthscales of variation in a mushy layer are dominated by thermal diffusion, solutal diffusion can be ignored in the macroscopic model of the interior of a mushy layer. We shall assume that the bulk composition of the mushy layer remains uniform at C_0 : if any part of the mushy layer becomes completely molten then the resulting melt will also have concentration C_0 . Note, however, that the concentration of the interstitial liquid is not uniform but determined by the liquidus given the local temperature.

In order to simplify the following presentation, we assume that the densities and specific heat capacities of the solid and liquid elements are the same, $\rho_l = \rho_s = \rho$ and $c_l = c_s = c$, respectively. We choose to scale the local conservation Eqs. (2) and (4) with a velocity scale V and the thermal diffus-

ivity $\kappa = k/(\rho c)$. Lengths are scaled with κ/V and times are scaled with κ/V^2 . With these scalings, the conservation equations combined with the liquidus constraint and the assumption of no solutal diffusion become

$$\frac{\partial}{\partial t}(\theta - \mathcal{S}\phi) = \nabla^2\theta \quad (5)$$

and

$$\frac{\partial}{\partial t}[(1 - \phi)\theta + \mathcal{C}\phi] = 0. \quad (6)$$

We have introduced the dimensionless temperature and concentration

$$\theta = \frac{T - T_L(C_0)}{\Delta T} = \frac{C - C_0}{\Delta C}, \quad (7)$$

where $\Delta T = T_L(C_0) - T_E$ and $\Delta C = C_0 - C_E$. The dimensionless melting temperature of the mushy layer is $\theta = 0$; above this temperature the mushy layer becomes completely molten. The dimensionless eutectic temperature of the mushy layer is $\theta = -1$; below this temperature the mushy layer forms a eutectic solid. The dimensionless parameters are the Stefan number

$$\mathcal{S} = \frac{\mathcal{L}}{c\Delta T} \quad (8)$$

and the compositional ratio

$$\mathcal{C} = \frac{C_s - C_0}{C_0 - C_E}, \quad (9)$$

where the composition of the solid C_s is constant. The Stefan number \mathcal{S} represents a balance between the latent heat release \mathcal{L} and sensible heat $c\Delta T$ potentially available in a mushy layer. The compositional ratio \mathcal{C} relates the difference in the composition of the solid and melt phases to the potential compositional variation within the melt phase across a mushy layer.

In this paper we consider one-dimensional situations only; we work in one spatial dimension (coordinate z) and combine Eqs. (5) and (6) to obtain

$$\left(1 + \frac{\mathcal{S}\mathcal{C}}{(\mathcal{C} - \theta)^2}\right) \frac{\partial\theta}{\partial t} = \frac{\partial^2\theta}{\partial z^2} \quad (10)$$

and

$$\phi = \frac{\theta}{\theta - \mathcal{C}}, \tag{11}$$

because of our assumption that the bulk composition is uniform. Note that our assumptions of thermodynamic equilibrium and zero solutal diffusion within the mushy layer have led us to an equation, Eq. (10), describing heat transfer through a medium with a thermal diffusivity that is a function of temperature.

3. Melting from a hot plate

Consider the one-dimensional system in Fig. 1. We use a Cartesian coordinate system with its origin fixed in the plate and with the z -axis increasing into the mushy layer. At times $t < 0$, the plate is in thermodynamic equilibrium with the mushy layer at temperature θ_∞ which is taken to be between the melting and freezing temperatures of the mushy layer. At $t = 0$, the temperature of the plate switches discontinuously to a new temperature θ_i . If $\theta_i > 0$ then part of the mushy layer will melt completely into a melt region with uniform concentration C_0 . If $0 > \theta_i > \theta_\infty$ then the mushy layer will

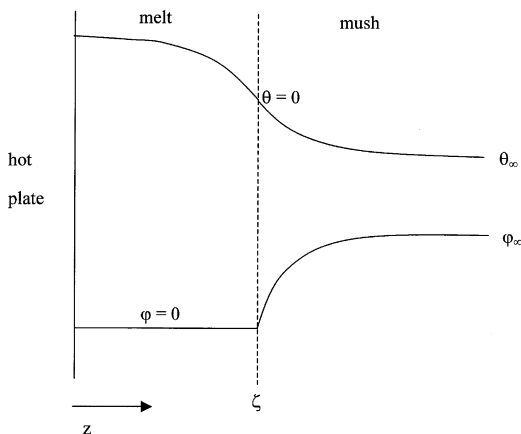


Fig. 1. A schematic diagram of a mushy layer brought into contact with a hot plate. At $t = 0$ the plate temperature discontinuously switches to θ_i . If $\theta_i > 0$ then the melt forms.

melt, decreasing its solid fraction, but no completely molten region will be generated. If $\theta_\infty > \theta_i > -1$, then the mushy layer will freeze by increasing its solid fraction but will not become completely solid. Finally, if $\theta_i < -1$, then part of the mushy layer freezes completely to form a eutectic solid. We confine our attention to the cases in which melting occurs and consider first the situation in which $\theta_i < 0$ so that no completely molten region is formed.

3.1. No melt generated, $\theta_i < 0$

The equations describing the evolution of the mushy layer are Eqs. (10) and (11). The boundary conditions for $t > 0$ are

$$\theta = \theta_i \quad (z = 0), \tag{12}$$

$$\theta \rightarrow \theta_\infty \quad (z \rightarrow \infty), \tag{13}$$

This implies that

$$\phi_\infty = \lim_{z \rightarrow \infty} \phi = \frac{-\theta_\infty}{\mathcal{C} - \theta_\infty} \tag{14}$$

The solid fraction of the mushy layer in contact with the plate is $\phi(z = 0) = -\theta_i/(\mathcal{C} - \theta_i)$.

This problem admits a similarity solution $\theta(z, t) = \theta(\eta)$, where the similarity variable is $\eta = zt^{-1/2}$. Searching for this solution reduces Eq. (10) to an ordinary differential equation. The reduced problem becomes

$$-\frac{1}{2}\eta\theta' \left(1 + \frac{\mathcal{S}\mathcal{C}}{(\mathcal{C} - \theta)^2} \right) = \theta'', \tag{15}$$

subject to

$$\theta = \theta_i \quad (\eta = 0), \tag{16}$$

$$\theta \rightarrow \theta_\infty \quad (\eta \rightarrow \infty), \tag{17}$$

where $\phi(\eta)$ is given by Eq. (11). Eq. (15) was solved numerically using the method of shooting.

In addition, we examined a simple asymptotic limit. Suppose $\mathcal{C} \gg 1$, $\mathcal{S} \gg 1$ with \mathcal{S}/\mathcal{C} of $\mathcal{O}(1)$ and (by assumption) θ is of $\mathcal{O}(1)$, see [9]. Then, Eq. (15) approximates to

$$-\frac{1}{2}\eta\Omega\theta' = \theta'', \tag{18}$$

where

$$\Omega = 1 + \frac{\mathcal{S}}{\mathcal{C}}. \quad (19)$$

This equation is linear and admits an analytical solution. Integrating Eq. (18) twice and applying the boundary conditions (16) and (17) yields the solution

$$\theta = \theta_i + (\theta_\infty - \theta_i)\text{erf}(\Omega^{1/2}\eta/2), \quad (20)$$

where $\text{erf}(x)$ is the error function given by

$$\text{erf}(x) = \frac{2}{\sqrt{\pi}} \int_0^x e^{-s^2} ds \quad (21)$$

and ϕ is given by Eq. (11).

The solutions for θ and ϕ are plotted in Fig. 2 for $\theta_i = -0.1$, $\theta_\infty = -0.5$, $\mathcal{S} = 1$ and $\mathcal{C} = 1$. The

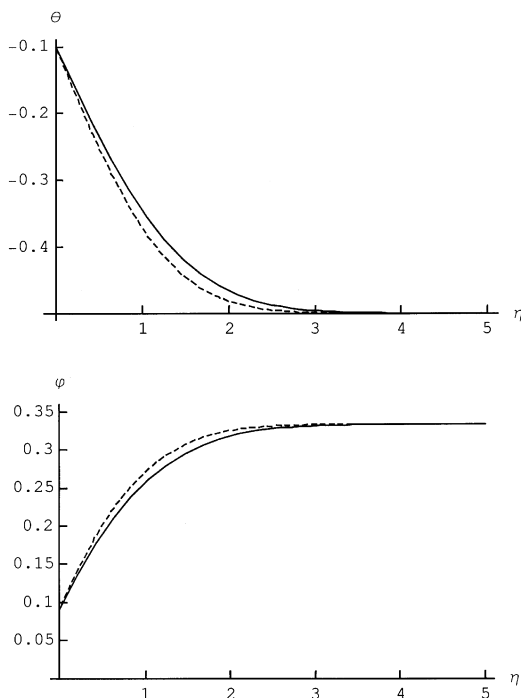


Fig. 2. Temperature θ and solid fraction ϕ within the mushy layer for $\theta_i = -0.1$, $\theta_\infty = -0.5$, $\mathcal{S} = 1$ and $\mathcal{C} = 1$. The solid line shows the solution to the full nonlinear problem, the dashed line shows the solution to the asymptotic problem.

solution to the full nonlinear problem (obtained numerically) is shown with a solid line, the solution to the asymptotic problem is shown with a dashed line. The asymptotic problem relies on the limit $\mathcal{C} \gg 1$, $\mathcal{S} \gg 1$ yet the error is less than 10%. Throughout this paper, we shall present the true solutions together with the solutions obtained using the asymptotic limit. Since we take $\mathcal{C} = 1$ and $\mathcal{S} = 1$ throughout, the difference between the true and asymptotic solutions can be viewed as an upper limit to the inaccuracy of the asymptotic approximation. For many materials $\mathcal{C} \gg 1$, $\mathcal{S} \gg 1$ and the asymptotic approximation is excellent. Fig. 3 shows solutions to the full nonlinear problem with $\theta_i = -0.1$, $\theta_\infty = -0.5$, $\mathcal{S} = 1$ and $\mathcal{C} = 1$ (solid line), $\mathcal{S} = 10$ and $\mathcal{C} = 1$ (dashed line), and $\mathcal{S} = 1$ and $\mathcal{C} = 100$ (dotted line). We see that increasing the Stefan number \mathcal{S} decreases the extent

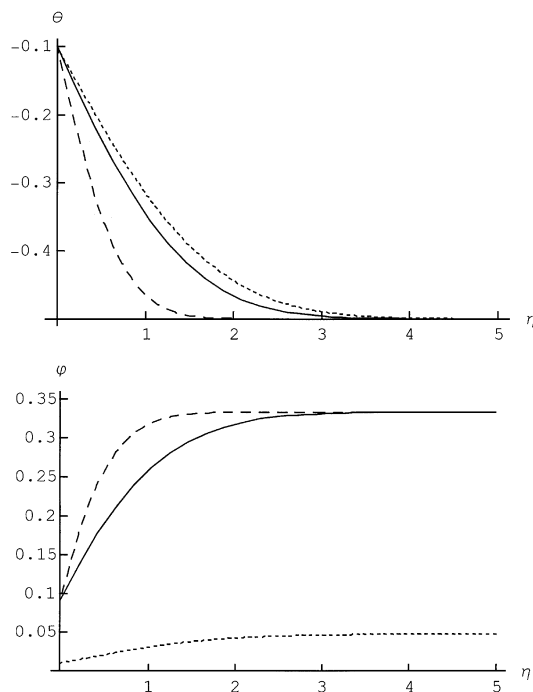


Fig. 3. Solutions of the full nonlinear problem for temperature θ and solid fraction ϕ within the mushy layer for $\theta_i = -0.1$, $\theta_\infty = -0.5$, $\mathcal{S} = 1$ and $\mathcal{C} = 1$ (solid line), $\mathcal{S} = 10$ and $\mathcal{C} = 1$ (dashed line), and $\mathcal{S} = 1$ and $\mathcal{C} = 100$ (dotted line).

of temperature and phase change, and increasing the compositional ratio \mathcal{C} has little effect on the temperature profiles but decreases the volume of material undergoing phase change. Increasing \mathcal{S} is equivalent to increasing the latent heat \mathcal{L} ; more energy is required to dissolve solid elements and more energy is released on freezing the liquid elements of the mushy layer. This acts to weaken the effect of the imposed temperature θ_i . Increasing \mathcal{C} is equivalent to steepening the liquidus curve, which implies a smaller amount of phase change is required to keep the interstitial liquid on the liquidus.

3.2. Melt generated, $\theta_i > 0$

We now consider the situation in which at $t = 0$, the temperature of the plate is increased discontinuously to a temperature above the liquidus temperature at the bulk composition $\theta_i > 0$ and a melt region forms with the position of the mush–melt interface at $z = \zeta(t)$.

The equations describing the mushy layer are Eqs. (10) and (11). The equation describing conservation of heat in the melt is

$$\frac{\partial \theta}{\partial t} = \frac{\partial^2 \theta}{\partial z^2}. \quad (22)$$

Since the composition of the mushy layer is uniform, there is no concentration variation in the melt formed and thus no solutal diffusion. The boundary conditions at $t > 0$ are Eq. (12),

$$\theta = 0 \quad (z = \zeta(t)) \quad (23)$$

$$[\theta]_\ell^m = 0 \quad (z = \zeta(t)), \quad (24)$$

$$\mathcal{S} \phi \frac{\partial \zeta}{\partial t} = \left[\frac{\partial \theta}{\partial z} \right]_\ell^m \quad (z = \zeta(t)), \quad (25)$$

and Eq. (13) where $[\dots]_\ell^m$ denotes the difference in the enclosed quantity between the mushy layer m and melt ℓ . Note that (23) combined with (11) implies that $\phi = 0$ at the interface which is consistent with the general set of boundary conditions derived by Schulze and Worster [10] since, relative to the phase boundary, the liquid flows from mush to liquid. This reduces the Stefan condition (25) to continuity of heat flux; this condition determines

the motion of the mush–melt interface. We search for the similarity solution $\theta(z, t) = \theta(\eta)$ with the mush–melt interface position given by $\zeta = \lambda t^{1/2}$, where λ is an eigenvalue determined from the Stefan condition. In the similarity variable, the problem becomes Eq. (15) in the mushy layer and

$$-\frac{1}{2}\eta\theta' = \theta'' \quad (26)$$

in the melt, subject to Eq. (16),

$$\theta = 0, \quad (\eta = \lambda), \quad (27)$$

$$[\theta]_\ell^m = 0 \quad (\eta = \lambda), \quad (28)$$

$$[\theta']_\ell^m = 0 \quad (\eta = \lambda) \quad (29)$$

and Eq. (17). The solid fraction is given by Eq. (11).

The solution in the melt is simply obtained from integration and application of boundary conditions to be

$$\theta = \theta_i \left(1 - \frac{\text{erfc}(\eta/2)}{\text{erfc}(\lambda/2)} \right). \quad (30)$$

Again, we consider the asymptotic problem with Eq. (15) replaced with Eq. (18). The solution to this approximate system is found from integration and application of boundary conditions to be

$$\theta = \theta_\infty \frac{(\text{erfc}(\Omega^{1/2}\eta/2) - \text{erfc}(\Omega^{1/2}\lambda/2))}{\text{erfc}(\Omega^{1/2}\lambda/2)}, \quad (31)$$

where $\text{erfc}(x)$ is the complementary error function, $\text{erfc}(x) = 1 - \text{erf}(x)$, and ϕ is given by Eq. (11). Application of the Stefan condition (29) yields the transcendental equation

$$\theta_\infty \frac{\Omega^{1/2} e^{-\Omega\lambda^2/4}}{\text{erfc}(\Omega^{1/2}\lambda/2)} = -\theta_i \frac{e^{-\lambda^2/4}}{\text{erfc}(\lambda/2)}, \quad (32)$$

which determines the eigenvalue λ .

We solved the full nonlinear problem consisting of Eq. (15) subject to Eq. (27) and (17) numerically. We integrate from the initial conditions

$$\theta = 0, \theta' = g_j \quad (\eta = \lambda^*), \quad (33)$$

to match the condition $\theta \rightarrow \theta_\infty$ as $\eta \rightarrow \infty$. Once we converge on θ_∞ then $g_n = g_*(\lambda^*)$ is recorded. This quantity $g_*(\lambda^*) = \theta'(\eta = \lambda^*)$ is the dimensionless diffusional heat flux from the mushy layer at the

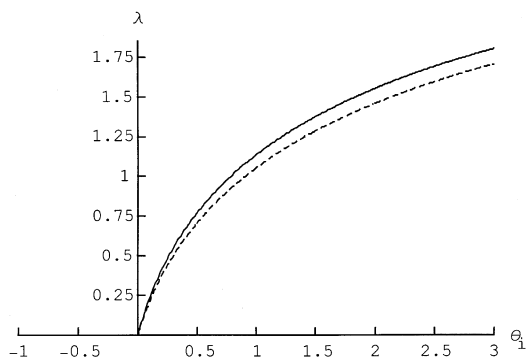


Fig. 4. Variation of λ with θ_i for $\theta_\infty = -0.5$, $\mathcal{S} = 1$ and $\mathcal{C} = 1$. The solid line shows the solution to the full nonlinear problem, the dashed line shows the solution to the asymptotic problem. There is no solution shown for $\theta_i < 0$ because then no melt region is generated and the model is inappropriate.

mush–melt interface and is used in the Stefan condition. The procedure is automated and repeated to obtain the curve $g_*(\lambda)$. In terms of g_* , the Stefan condition (29) can be rewritten

$$g_* = g_*(\lambda; \mathcal{S}, \mathcal{C}, \theta_\infty) = Y, \quad (34)$$

where

$$Y = Y(\lambda, \theta_i) = -\frac{\theta_i e^{-\lambda^2/4}}{\sqrt{\pi} \operatorname{erf}(\lambda/2)}. \quad (35)$$

Eq. (34) is the transcendental equation determining the eigenvalue λ . Since g_* is independent of θ_i and Y is expressed in closed form, we can calculate the dependence of λ on θ_i using repeated root-finding with the secant method. In Fig. 4, we show $\lambda(\theta_i)$ for $\mathcal{S} = 1$, $\mathcal{C} = 1$ and $\theta_\infty = -0.5$. The asymptotic solution (the dashed line) was obtained from Eq. (32) using a Newton–Raphson root-finder. For $\theta_i \geq 0$, there exists a solution $\lambda \geq 0$ corresponding to an evolving mush–melt boundary. For $\theta_i < 0$, there is no solution for λ . This is because no melt region is generated and the model is inappropriate; where there is no melt region we use the equations of the previous section. We plot the solutions θ and ϕ in Fig. 5 for $\theta_i = 0.5$, $\theta_\infty = -0.5$, $\mathcal{S} = 1$ and $\mathcal{C} = 1$.

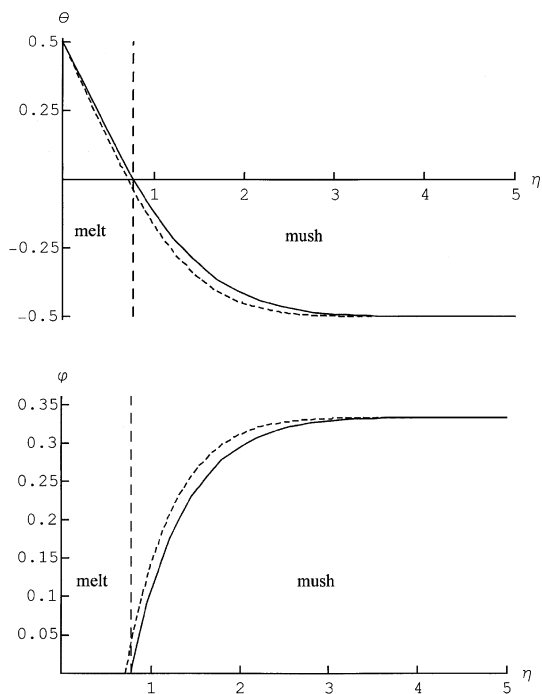


Fig. 5. Temperature θ and solid fraction ϕ in the mushy layer and melt for $\theta_i = 0.5$, $\theta_\infty = -0.5$, $\mathcal{S} = 1$ and $\mathcal{C} = 1$. The solid line shows the solution to the full nonlinear problem, the dashed line shows the solution to the asymptotic problem.

4. Mushy layer in contact with a hot liquid

Consider the one-dimensional system in Fig. 6 in which a mushy layer is in contact with a liquid. Before $t = 0$, the mushy layer is of uniform temperature θ_∞ , bulk composition C_0 and hence solid fraction ϕ_∞ . There is no melt region. We consider the physical properties of the liquid to be identical to the melt generated as the mushy layer becomes completely molten. Thus, there is no solutal diffusion in the liquid region. We set the far-field temperature in the liquid to be $\theta_{-\infty} > 0$ and calculate the evolution of this system after $t = 0$. A Cartesian coordinate system is used with the origin of z fixed at the position of the mush–melt–liquid interface at time $t < 0$, with z increasing into the mushy layer.

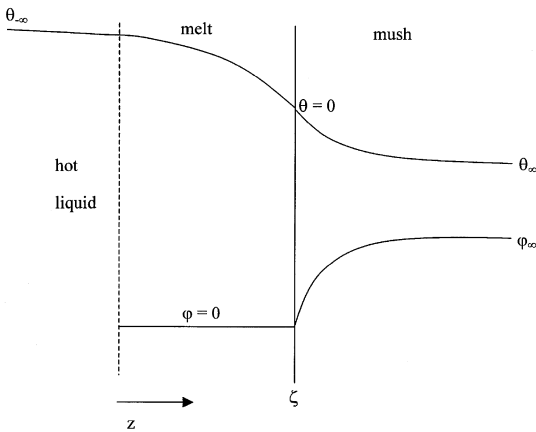


Fig. 6. A schematic diagram of a mushy layer brought into contact with a hot melt. The melt may form due to the hot liquid dissolving the mushy layer after $t = 0$.

We search for a similarity solution in the similarity variable $\eta = zt^{-1/2}$, with the mush–melt interface located at $\zeta(t) = \lambda t^{1/2}$. The equations describing the mushy layer are (15) and (11), the equation describing the liquid and melt is (26). The boundary conditions are

$$\theta \rightarrow \theta_{\infty} \quad (\eta \rightarrow -\infty), \tag{36}$$

Eqs. (27)–(29) and (17). The solution in the melt region is obtained straightforwardly by integration of the governing equation and applying boundary conditions to be

$$\theta = \theta_{\infty} \frac{(\text{erf}(\lambda/2) - \text{erf}(\eta/2))}{1 + \text{erf}(\lambda/2)}. \tag{37}$$

The problem of obtaining the temperature (and hence solid fraction) in the mushy layer is identical to that presented in the preceding section. The equation determining λ , however, is modified by the solution in the liquid–melt region to

$$g_* = \tilde{\gamma}, \tag{38}$$

where

$$\tilde{\gamma} = -\frac{\theta_{\infty}}{\sqrt{\pi}} \frac{e^{-\lambda^2/4}}{1 + \text{erf}(\lambda/2)}. \tag{39}$$

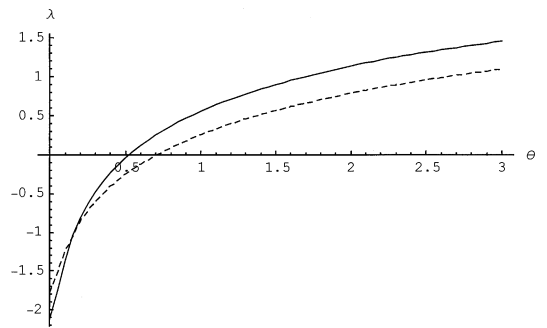


Fig. 7. Variation of λ with $\theta_{-\infty}$ for $\theta_{\infty} = -0.5$, $\mathcal{S} = 1$ and $\mathcal{C} = 1$. The solid line shows the solution to the full nonlinear problem, the dashed line shows the solution to the asymptotic problem.

The variation of λ with $\theta_{-\infty}$ is calculated using repeated root-finding. In Fig. 7, we plot $\lambda(\theta_{-\infty})$ for $\mathcal{S} = 1$, $\mathcal{C} = 1$ and $\theta_{\infty} = -0.5$. There exists a critical temperature $\theta_{-\infty}^{\text{crit}}$, below which $\lambda < 0$ and the mushy layer advances into the liquid by freezing.

We can easily determine the variation of $\theta_{-\infty}^{\text{crit}}$ with θ_{∞} . The value of $\theta_{-\infty}^{\text{crit}}$ is given by Eq. (38) with $\lambda = 0$, rearranging and substituting for $\tilde{\gamma}$ yields

$$\theta_{-\infty}^{\text{crit}}(\theta_{\infty}) = -\sqrt{\pi} g_*(\theta_{\infty}; \lambda = 0), \tag{40}$$

where $g_*(\theta_{\infty}; \lambda = 0)$ is obtained numerically using shooting. We can estimate $\theta_{-\infty}^{\text{crit}}$ analytically by considering the asymptotic equation for the mushy layer (18). Solving this equation subject to Eqs. (27) and (17) gives the temperature in the mushy layer to be

$$\theta = \theta_{\infty} \frac{(\text{erf}(\Omega^{1/2}\eta/2) - \text{erf}(\Omega^{1/2}\lambda/2))}{\text{erfc}(\Omega^{1/2}\lambda/2)}, \tag{41}$$

with ϕ given by Eq. (11). Application of the Stefan condition (29) yields the transcendental equation

$$\frac{\theta_{-\infty} e^{-\lambda^2/4}}{1 + \text{erf}(\lambda/2)} + \frac{\theta_{\infty} \Omega^{1/2} e^{-\Omega\lambda^2/4}}{\text{erfc}(\Omega^{1/2}\lambda/2)} = 0. \tag{42}$$

This equation was used to calculate the asymptotic dependence of λ upon $\theta_{-\infty}$ shown in Fig. 7 for

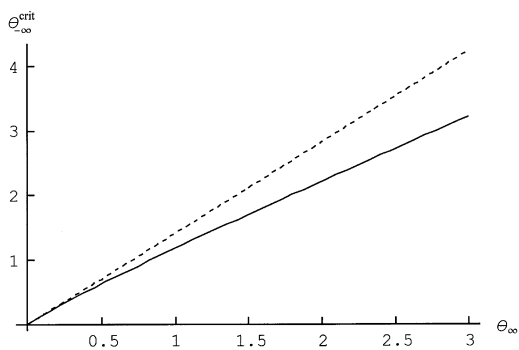


Fig. 8. Variation of $\theta_{-\infty}^{\text{crit}}$ with θ_{∞} for $\mathcal{S} = 1$ and $\mathcal{C} = 1$. The solid line shows the solution to the full nonlinear problem, the dashed line shows the solution to the asymptotic problem.

$\mathcal{S} = 1$, $\mathcal{C} = 1$ and $\theta_{\infty} = -0.5$. Setting $\lambda = 0$, we obtain

$$\theta_{-\infty}^{\text{crit}} = -\Omega^{1/2}\theta_{\infty}. \tag{43}$$

In Fig. 8, we plot $\theta_{-\infty}^{\text{crit}}$ versus θ_{∞} for $\mathcal{S} = 1$ and $\mathcal{C} = 1$. The asymptotic problem badly over-estimates $\theta_{-\infty}^{\text{crit}}(\theta_{\infty})$ at large θ_{∞} but numerical studies show that the approximation greatly improves as \mathcal{C} is increased into the appropriate asymptotic regime of $\mathcal{C} \gg 1$. We plot the solutions θ and ϕ in Fig. 9 for $\mathcal{S} = 1$, $\mathcal{C} = 1$, $\theta_{\infty} = -0.5$ and $\theta_{-\infty} = 1.0$.

5. Investigation of internal phase change and discussion

We consider the case of a mushy layer in contact with a hot liquid since this system exhibits behaviour which encompasses that of the simpler systems. We investigate the extent and volume of the internal phase change within the mushy layer and contrast the melting behaviour with that of a pure material. A full exploration of the realistic parameter regimes would be infeasible; we concentrate here upon the effect of varying the far-field temperature in the hot liquid.

Consider Fig. 10, which is plotted for $\mathcal{S} = 1$, $\mathcal{C} = 1$ and $\theta_{\infty} = -0.5$. The solid line shows the total volume of phase change $M_T = M_I + \lambda\phi_{\infty}$,

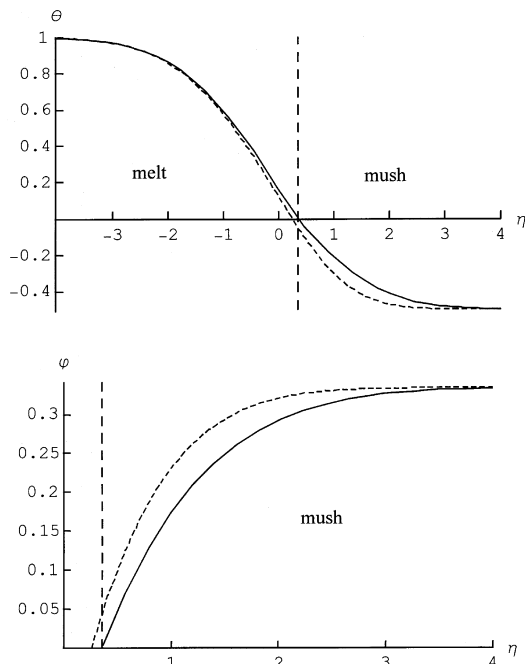


Fig. 9. The temperature θ and solid fraction ϕ in the mushy layer and melt for $\theta_{-\infty} = 1.0$, $\theta_{\infty} = -0.5$, $\mathcal{S} = 1$ and $\mathcal{C} = 1$. The solid line shows the solution to the full nonlinear problem, the dashed line shows the solution to the asymptotic problem.

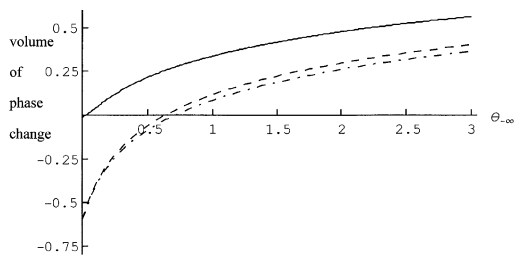


Fig. 10. Variation of the volume of phase change with $\theta_{-\infty}$ for $\theta_{\infty} = -0.5$, $\mathcal{S} = 1$ and $\mathcal{C} = 1$. The solid line shows the total phase change, M_T ; the dashed line shows $\lambda\phi_{\infty}$; and the dashed-dotted line shows $\lambda_{\text{ps}}\phi_{\infty}$.

where $M_I = \int_{\lambda}^{\infty} (\phi_{\infty} - \phi) d\eta$ is that melted internally and is calculated using shooting and numerical quadrature. The dashed line shows $\lambda\phi_{\infty}$ which, for the melting values of $\theta_{-\infty}$ (λ positive), equals the

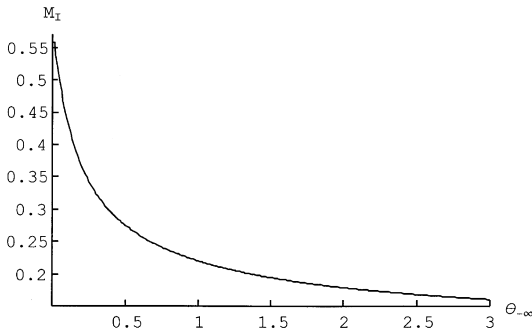


Fig. 11. Variation of the volume of internal phase change M_I with $\theta_{-\infty}$ for $\theta_{\infty} = -0.5$, $\mathcal{S} = 1$ and $\mathcal{C} = 1$.

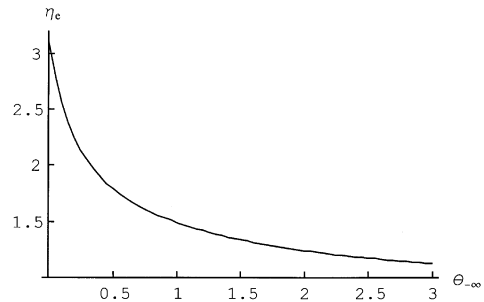


Fig. 12. Variation of the extent of internal phase change η_e with $\theta_{-\infty}$ for $\theta_{\infty} = -0.5$, $\mathcal{S} = 1$ and $\mathcal{C} = 1$.

volume of mushy layer that becomes completely molten. Negative values of $\lambda\phi_{\infty}$ correspond to freezing of the hot liquid, which increases the depth of the mushy layer. The difference between the total phase change curve and $\lambda\phi_{\infty}$ is the volume of internal phase change, M_I . From Fig. 11, we see that the volume of internal phase change within the mushy layer decreases as $\theta_{-\infty}$ increases. The extent of the internal phase change within the mushy layer is also of interest; we define η_e from $\phi(\eta = \lambda + \eta_e) = \frac{9}{10}\phi_{\infty}$, the depth within the mushy layer at which the solid fraction reaches $\frac{9}{10}$ of its far-field value. From Fig. 12, we see that the extent of internal phase change decreases as $\theta_{-\infty}$ increases. In Fig. 10, the dashed-dotted curve is $\lambda_{ps}\phi_{\infty}$, where λ_{ps} is the position of a pure solid–melt interface. The value of λ_{ps} is determined as part of the classical melting Stefan problem given by (10) with $\mathcal{C} \rightarrow \infty$ subject to Eqs. (36), (23)–(25), with $\phi \rightarrow 1$ and Eq. (13), see [4]. As $\theta_{-\infty}$ increases, $\lambda\phi_{\infty}$ approaches $\lambda_{ps}\phi_{\infty}$, this is because the volume and extent of phase change within the mushy layer decreases as $\theta_{-\infty}$ increases. From these results it is clear that internal melting can be significant for both melting and freezing mushy layers and becomes less significant in strong melting conditions ($\theta_{-\infty} \gg \theta_{-\infty}^{crit}$).

An example of a mushy layer in which internal phase change is of importance is sea ice, which is well approximated by ice formed from aqueous solutions of sodium-chloride [11]. As sea ice melts internally its solid fraction decreases which dimin-

ishes its strength and can allow break-up under the stresses imposed by the wind and ocean. A decrease in the solid fraction of sea ice also increases its permeability (a measure of its resistance to internal flows). This may promote significant brine flows and flushing of fresh water through the sea ice from the melting of snow and ice at its surface. These flows desalinate the sea ice and enhance the freshwater flux into the North Atlantic. More details about sea ice can be found in [8]; a discussion of mushy layers applied to sea ice can be found in Refs. [11,12].

6. Conclusions

In this paper, we have presented some solutions of the equations describing local conservation of heat and solute in a mushy layer and melt in the absence of flow. This section summarises our main conclusions.

A mushy layer can be partially melted from a plate without generation of a completely molten region by altering its solid fraction. Increasing the Stefan number \mathcal{S} decreases the region of substantial phase change and temperature variation. Increasing the composition ratio \mathcal{C} decreases the volume of material undergoing phase change.

Increasing the temperature of a plate in contact with a mushy layer above its melting point causes part of the mushy layer to melt completely. The higher the plate temperature above the melting

point, the more rapidly the melt–mush interface advances into the mushy layer. The solid fraction of the mushy layer at the mush–melt interface is zero.

A mushy layer placed in contact with a hot liquid with fixed far-field temperature can shrink or grow. The critical value of the far-field temperature in the liquid below which the mushy layer grows has been calculated.

The equations describing local conservation of heat and solute in the mushy layer can be decoupled and the asymptotic limit $\mathcal{C} \gg 1$, $\mathcal{S} \gg 1$ with \mathcal{C}/\mathcal{S} of $\mathcal{O}(1)$ taken which gives a linear equation for temperature that yields an analytical solution. We have plotted the asymptotic solutions for $\mathcal{C} = 1$ and $\mathcal{S} = 1$ in order to indicate an upper limit to the inaccuracy of the asymptotic approximation. For many materials $\mathcal{C} \gg 1$, $\mathcal{S} \gg 1$ and, in these cases, the asymptotic solutions are an excellent approximation.

The extent and volume of internal phase change within a mushy layer can be significant during both melting and freezing, and decreases during strong melting conditions. Internal phase change decreases the solid fraction of the mushy layer, which can weaken it, and increases its permeability, enhancing flows of the internal melt.

Acknowledgements

The work of M.G.W. is supported by the Natural Environmental Research Council.

References

- [1] H.E. Huppert, *J. Fluid Mech.* 212 (1990) 209.
- [2] M.G. Worster, *The dynamics of mushy layers*, volume 219 of NATO Advanced Study Institutes Series E, Applied Sciences, Kluwer Academic Publishers, Dordrecht, 1992, pp. 113–138.
- [3] A.W. Woods, *J. Fluid Mech.* 239 (1992) 429.
- [4] H.S. Carslaw, J.C. Jaeger, *Conduction of Heat in Solids*, Oxford University Press, Oxford, 1959.
- [5] M.G. Worster, *J. Fluid Mech.* 167 (1986) 481.
- [6] G.K. Batchelor, *Ann. Rev. Fluid Mech.* 6 (1974) 227.
- [7] A. Hellawell, J.R. Sarazin, R.S. Steube, *Phil. Trans. Roy. Soc. Lond. A.* 345 (1993) 507.
- [8] W.F. Weeks, S.F. Ackley, *The Geophysics of Sea Ice*, NATO Advanced Study Institutes Series B, Physics, Plenum Press, New York 1986, Vol. 146 (chapter 1).
- [9] P.W. Emms, A.C. Fowler, *J. Fluid Mech.* 262 (1994) 111.
- [10] T.P. Schulze, M.G. Worster, *J. Fluid Mech.* 388 (1999) 197.
- [11] J.S. Wettlaufer, M.G. Worster, H.E. Huppert, *Geophys. Res. Lett.* 24 (1997) 1251.
- [12] D.L. Feltham, *Fluid dynamics and thermodynamics of sea ice*, Ph.D. Thesis, University of Cambridge, 1997.